Drug Discovery

DOI: 10.1002/anie.200903821

Application of Fragment Growing and Fragment Linking to the Discovery of Inhibitors of *Mycobacterium tuberculosis* Pantothenate Synthetase**

*Alvin W. Hung, H. Leonardo Silvestre, Shijun Wen, Alessio Ciulli, Tom L. Blundell, and Chris Abell**

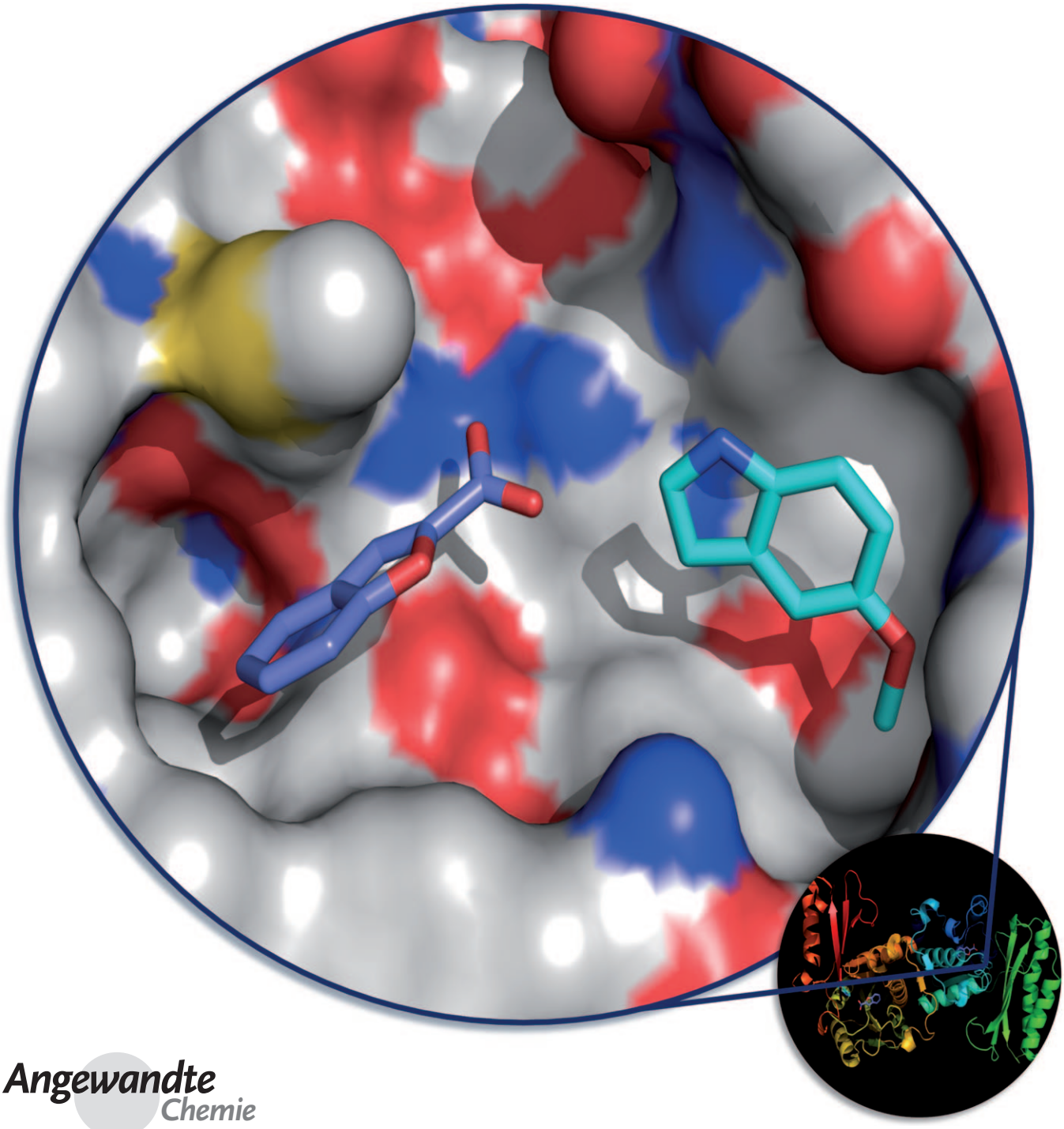

Despite the fact that nearly 2 million people a year are killed by *Mycobacterium tuberculosis* (TB),[1] we still lack a robust pipeline of potential therapies to combat this burden.[2] Fragment-based approaches[3–5] have provided a new paradigm in the development of high-quality chemical ligands and have great potential to contribute as starting points in the development of drugs against TB.[6]

Pantothenate synthetase (PS), the product of the *panC* gene, catalyzes the magnesium adenosine triphosphate (ATP) dependent condensation of pantoate with β-alanine to form pantothenate (vitamin B_5).[7,8] A pantothenate auxotroph of *M. tuberculosis* defective in the *panC* and *panD* genes was found to be highly attenuated in a mouse model of the disease.[9] This observation provides a level of genetic validation of the use of PS as a target for the development of new TB therapeutics. To date, studies on PS inhibition have focused on the synthesis of analogues of the pantoyl adenylate reaction intermediate[10,11] or the identification of hits from high-throughput screening.[12,13] Herein, we describe a combination of fragment-growing and fragment-linking approaches that led to the discovery of a new series of inhibitors of *M. tuberculosis* PS for the further validation of PS as a potential drug target for TB.

We devised a systematic strategy for fragment screening, validation, and characterization[14] for which a series of biophysical techniques were required, including a thermal-shift assay, ligand-based NMR spectroscopy, isothermal titration calorimetry (ITC), and X-ray crystallography (see Figure 1 in the Supporting Information). Once the binding modes of key fragments had been elucidated, compounds were designed and elaborated synthetically to enable additional interactions to be identified at the enzyme active site with the aid of computational docking experiments with GOLD (genetic optimization for ligand docking).[15] ITC and X-ray crystallographic experiments were then repeated on the elaborated fragments, and the process was iterated to increase ligand potency.

The compound 5-methoxyindole (**1**) was initially identified as an ATP-competitive hit by WaterLOGSY NMR spectroscopy.[16] ITC confirmed that the fragment bound with a K_D value of 1.1 mM and a ligand efficiency (LE)[17] of 0.36 (titrations for the compounds discussed are shown in Figures 6 and 7 in the Supporting Information). The precise binding mode was revealed by soaking the fragment into a crystal of PS and determining the structure by X-ray crystallography to a resolution of 1.6 Å (Figure 1a). The fragment was found to bind at the recognition site of the ATP adenine motif. Analysis of the crystal structure of **1** bound to PS revealed two key hydrogen-bonding interactions, one between the OMe group of the indole and the backbone nitrogen atom of Val187 and another between the indole NH group and a molecule of sulfate (present at 150 mM in the crystallization buffer), which itself interacts with the Ser197 backbone nitrogen atom and the Lys160 residue (see Figure 3a in the Supporting Information).

The screening of several fragments that were structurally closely related to **1** revealed a narrow structure–activity relationship for this fragment. For example, the replacement of the methoxy group with either a hydroxy group or a methyl group, or the replacement of the indole core with a benzopyridine or benzoimidazole heterocycle led to an at least 10-fold decrease in the binding affinity. These results demonstrated the importance of shape complementary and specificity in fragment binding (see Figure 2 in the Supporting Information). The initial fragment hit **1** was therefore selected to initiate a fragment-growing approach. The binding of the indole was enhanced by adding a carboxylic acid at C2 to give 5-methoxy-1*H*-2-carboxylic acid (**1a**; $K_D = 0.5$ mM, LE = 0.32) or by adding an alkyl carboxylic acid chain to the N1 position to give 2-(5-methoxy-1*H*-indol-1-yl)acetic acid (**1b**; $K_D = 0.5$ mM, LE = 0.30). The aim of both these modifications was to identify electrostatic interactions in the triphosphate-binding site for ATP. Crystal structures of **1a** and **1b** bound to the protein confirmed that the compounds recapitulate the binding mode observed for the initial hit **1**.

The carboxylate group of **1a** provided a handle for further elaboration of the fragment. Ester and amide groups were designed to extend the substituent at C2 of the indole. The resulting compounds, however, showed a significant decrease in LE (ca. 0.20) relative to that of the simpler indole fragments. The analysis of docked structures suggested that these compounds may be too planar and rigid to enable the ligand to bend into either the P1 (for pantoate binding) or P2 pockets (for pyrophosphate and β-alanine binding) of the active site without steric interaction with the surface around Met40. To avoid this clash, an acyl sulfonamide was incorporated into the inhibitor to "bend" it and thus enable it to fit into a binding pocket. This functional group would be partially deprotonated under physiological conditions; thus, electrostatic interactions with the side chain of His47 would be facilitated, as observed with **1a**. Compound **2** was found by ITC to bind with a K_D value of 210 μM (LE = 0.28). As evident from the crystal structure of **2** bound to PS, this fivefold increase in binding affinity relative to that of **1** can be

[*] A. W. Hung, Dr. S. Wen, Dr. A. Ciulli, Prof. C. Abell
Department of Chemistry, University of Cambridge
Lensfield Road, Cambridge CB2 1EW (UK)
Fax: (+44) 1223-336-362
E-mail: ca26@cam.ac.uk
Homepage: http://www.ch.cam.ac.uk/staff/ca.html
H. L. Silvestre, Prof. T. L. Blundell
Department of Biochemistry, University of Cambridge
80 Tennis Court Road, Cambridge CB2 1GA (UK)

[**] This research was supported by the Bill & Melinda Gates Foundation. We are also grateful for funding from the Agency for Science Technology and Research (A*star) Singapore (PhD sponsorship, A.W.H.), the Fundacao para a Ciencia e Tecnologia (FCT; PhD sponsorship, H.L.S.), and Homerton College (Junior Research Fellowship to A.C.).

Supporting information for this article, including details of the synthesis of all compounds on the basis of both the growing and the linking strategy, and details of the preparation and structure determination of all ligands bound to the macromolecule, is available on the WWW under http://dx.doi.org/10.1002/anie.200903821. The atomic coordinates and structure factors for enzyme–ligand complexes have been deposited in the Protein Data Bank (http://www.rcsb.org/pdb/) and have the following ID codes: **1**: 3IMC; **2**: 3ISJ; **3**: 3IUB; **4**: 3IUE; **5**: 3IME; **6**: 3IVC; **7**: 3IVG; **8**: 3IVX; **1**+**5**: 3IMG.

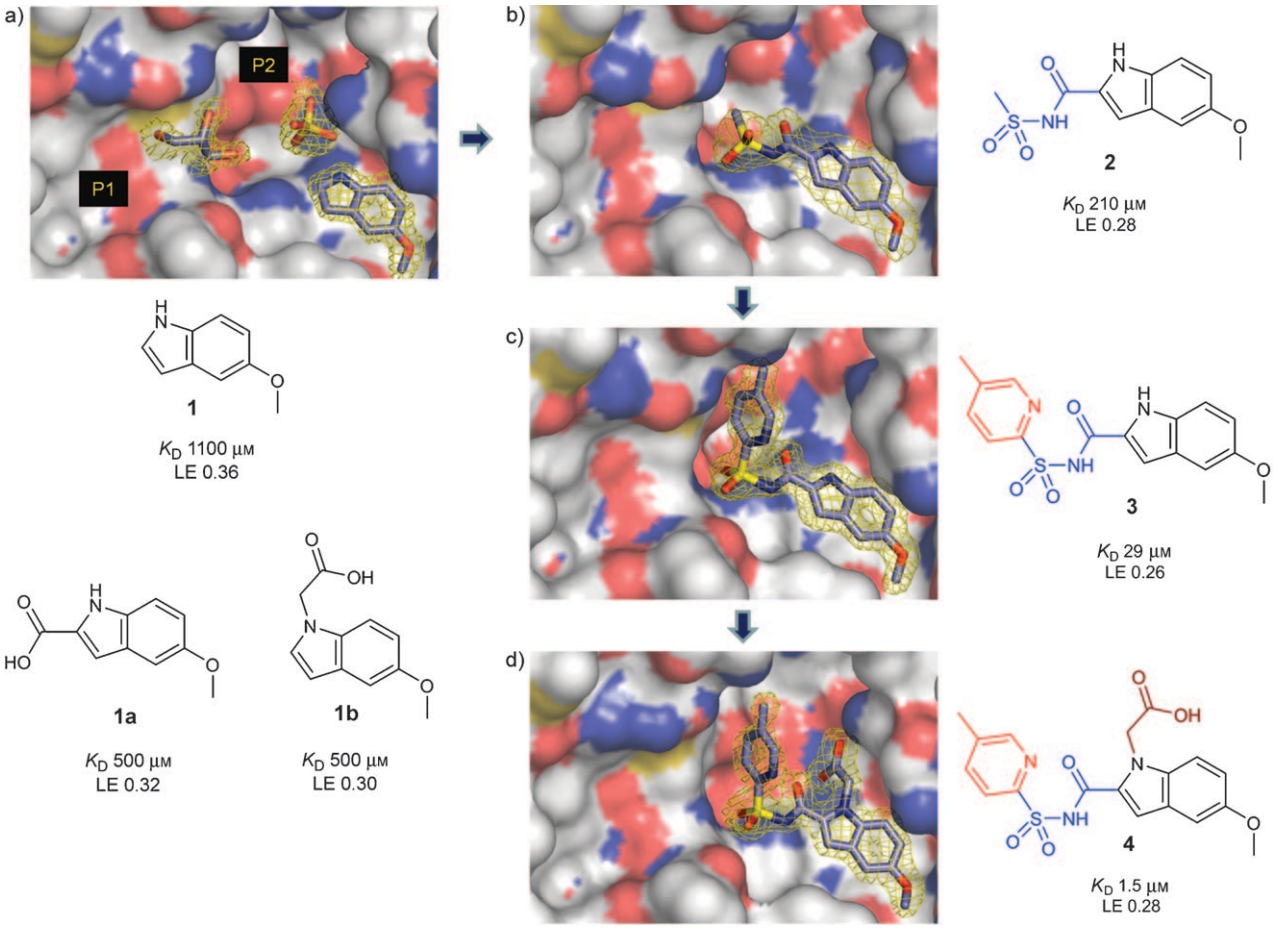

Figure 1. A fragment-growing strategy designed for *M. tuberculosis* pantothenate synthetase. a) The crystal structure of **1** bound together with sulfate and glycerol molecules reveals fragment-growing opportunities at both the C2 and N1 positions of the indole. Possible growth pockets are P1 (pantoate-binding site) and P2 (pyrophosphate-/β-alanine-binding site). Constructive modifications around the initial fragment generated compounds **1a** and **1b**. b) In compound **2**, an acyl sulphonamide was "grown" from the C2 position of the indole to enable elaboration into either P1 or P2. c) The elaboration of **2** generated compound **3**, which was found to bind in such a way that the 4-methylpyridine heterocycle filled the P2 pocket. d) Further growth from N1 of the indole generated the potent inhibitor **4**. The initial 5-methoxyindole fragment maintains its original position throughout the elaboration process; thus, this group is a suitable anchor core for growth. The $2F_o-F_c$ electron-density maps superimposed around each ligand are shown in yellow and contoured at 1σ. The ligands are shown as sticks with carbon atoms in blue, nitrogen atoms in darker blue, oxygen atoms in red, and sulfur atoms in yellow. The figures were generated and rendered with PyMOL v.0.99.[21]

attributed to additional hydrogen-bonding interactions between the sulfone oxygen atom and both the backbone amide group of Met40 and the side-chain nitrogen atom of His47. More importantly, as the methyl sulfonamide group is bent by approximately 90°, collision with the wall of the active site is avoided. The binding of **2** (Figure 1b) was also found to be consistent with the original binding mode of **1**, which confirmed that the initial indole fragment is a good anchor for fragment evolution.

The X-ray crystal structure of **2** bound to the protein suggested the possibility of further elaboration of the sulfonamide, for example, by growing along a vector leading either downwards into the P1 pocket or upwards into the P2 pocket. The introduction of a 4-methylpyridine ring on the sulphonamide gave **3** ($K_D = 29$ μM, LE = 0.26). The X-ray crystal structure of the binary complex of **3** with PS shows that the methylpyridine moiety occupies the binding site of β-alanine at the P2 pocket and forms hydrophobic interactions with the adjacent Tyr82 and Gln164 residues (Figure 1c). To increase the potency further, we introduced the alkyl carboxylic group in **1b** at the N1 position of the indole in **3**. On the basis of the previous elaboration of **1** to give **1b**, we expected that the carboxyl group would bind to the side chain of His44. This interaction was indeed observed; the sulphonamide carboxylic acid **4** (Figure 1d) had a K_D value of 1.5 μM and an LE value of 0.28. Compound **4** (see details of binding interactions in Figure 3b of the Supporting Information) was found to be an ATP-competitive inhibitor ($K_i = 27$ μM) of the enzyme in a coupled kinetic-inhibition assay.

Fragment **5** was identified from a thermal-shift screen[18] ($\Delta T_m = 1.6$ °C). The hit was confirmed by WaterLOGSY NMR spectroscopy and ITC ($K_D = 1$ mM, LE = 0.34). Interestingly, the X-ray crystal structure of **5** soaked into PS crystals showed that **5** binds across the P1 pocket, 3.1 Å away from the binding site of the indole **1**. Key interactions for **5** include hydrogen bonds from the carboxyl group to Met40 and His47 (see Figure 5a in the Supporting Information). Importantly, the crystal structure of **5** bound to PS suggested

that this compound may be able to bind to the active site simultaneously with fragment **1**, and so could be used in a linking strategy. To test this hypothesis, the two compounds were soaked as a cocktail into crystals of PS. The resulting electron-density map clearly showed the presence of both fragments in the active site. Their binding modes were similar to those of the individual compounds: minimal movement of the fragments from the positions of the individual compounds in the active site and minimal conformational changes were observed (Figure 2a).

Fragments **1** and **5** do not bind in the same plane (see Figure 5b in the Supporting Information). A flexible alkyl ester linking the C2 atoms of **1** and **5** was therefore designed to enable both fragments to adopt their original binding modes. The linked compound **6** binds an order of magnitude more tightly than either **1b** or **5** ($K_D = 75$ μM, LE = 0.20); however, the binding of **6** is much weaker than would be expected from complete additivity of the binding energies of the respective fragments. The X-ray crystal structure of **6** bound to PS (Figure 2b; see also Figure 4a in the Supporting Information) confirms the linking of the indole and benzofuran fragments. The molecule bends sharply to avoid the Met40 wall. Furthermore, the hydrogen bonds formed by the carboxyl group of **5** are lost, as this group has been replaced with the flexible alkyl portion of the ester linker. An alkyl sulfonamide linker was designed to incorporate a bend into the molecule and retain these crucial hydrogen bonds. To maintain linker flexibility, we attached a compensating methylene group to the indole fragment. Compound **7** (Figure 2c; see also Figure 4b in the Supporting Information) was found to bind with marginally improved affinity ($K_D =$ 50 μM, LE = 0.20).

To further improve the linker, an acyl sulfonamide group that had been employed successfully in the growth strategy (see above) was introduced. We believed it would be advantageous to restrict the additional flexibility introduced adjacent to the indole ring in compound **7**. The acyl sulfonamide moiety should still be able to bend to avoid the Met40 wall and thus adopt the correct conformation to place the benzofuran fragment in the P1 pocket. This hypothesis was supported by GOLD docking results. Compound **8** was therefore synthesized and was found to bind with significantly increased potency ($K_D = 1.8$ μM, LE = 0.26, $K_i = 9$ μM (competitive inhibition in the presence of ATP)). The crystal

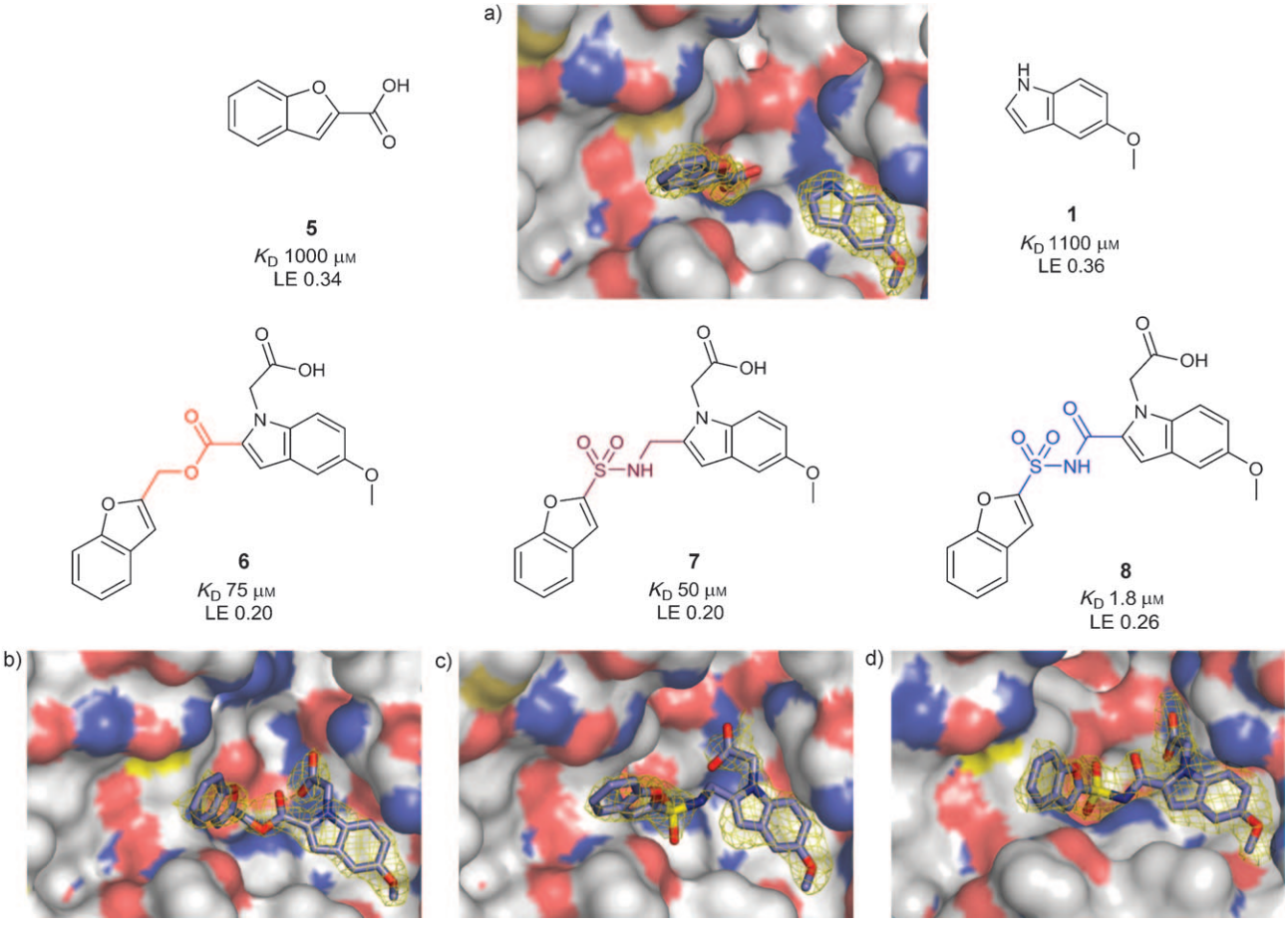

Figure 2. A fragment-linking strategy designed for *M. tuberculosis* pantothenate synthetase. a) Fragments **1** and **5**, soaked as a cocktail into crystals of PS, bind simultaneously at the active site; **5** occupies the P1 pocket. For clarity, a molecule of sulfate bound in the active site (modeled to 50% occupancy) is not shown. b,c) Crystal structures of ligands **6** and **7**, with an alkyl ester and a methylene sulphonamide linker group, respectively. Compounds **1** and **5** were linked successfully with these groups; however, a loss in LE was observed with respect to the initial fragments. d) Crystal structure of inhibitor **8**, which contains a more conformationally constrained acyl sulfonamide linker; in this case, the desired additivity of the binding energies of the initial fragments was observed. Electron-density maps and color coding as in Figure 1.

structure of **8** bound to PS (Figure 2d) shows that with the sulfamoyl linker the indole still binds in its original position; the compound bends to place the benzofuran group in the P1 pocket, and the hydrogen-bonding interactions with the Met40 residue are similar to those formed by the original fragment **5**. The benzofuran is slightly twisted relative to the position of **5**, which suggests that the constraints of the linker do not enable this moiety to adopt its optimum conformation (see Figures 4c and 5c in the Supporting Information).

It is interesting that although the indole acyl sulfonamide functionality in **4** and **8** is identical, the aryl ring on the sulfonamide occupies different pockets in the two final compounds. The linked structure **8** shows the expected binding of the two progenitor fragments. The binding of product **4** of the growth strategy is more surprising, as the aromatic substituent is in the P2 site. Overall, the LE values of inhibitors **2**–**4**, derived from fragment growing, are higher than those of **6**–**8**, which are derived from fragment linking. This result is characteristic of the two approaches.[14,19] The linking strategy is constrained by the size of the original fragments and that of the linker; it therefore results in a rapid buildup of atoms in a single step. Furthermore, conformational strain and flexibility mean that an energy price often needs to be paid to achieve optimal linking of fragments.[20] In contrast, the fragment-growing strategy permits the multistep optimization of ligand efficiency and size to enable a more flexible exploration of the binding site.

Through our fragment-based approaches, we very quickly developed millimolar potency fragments into potent inhibitors of *M. tuberculosis* pantothenate synthetase in a logical and direct way. The analysis of enzyme–ligand complexes and ligand efficiencies were also used to guide rational design during each synthetic cycle, so that incorrect assumptions were not built on during the optimization process. This process was particularly important for the growth strategy, in which extension up into the P2 pocket had not originally been expected. Likewise for the linking strategy, detailed structural analysis helped guide the choice of linkers and understanding of the conformational restraints they imposed. Furthermore, the study has enabled the direct comparison and contrast of fragment growing and fragment linking for the first time. The two strategies resulted in similar compounds with similar potencies. This outcome obscures the fact that although the linking strategy appears more elegant, the limited repertoire of linkers is likely to compromise the binding of the original fragments. In comparison, the fragment-growing strategy provides more freedom for development at each stage and allows more room for further optimization.

Received: July 13, 2009
Published online: September 24, 2009

Keywords: drug design · fragment linking · inhibitors · tuberculosis · X-ray diffraction

[1] E. L. Corbett, C. J. Watt, N. Walker, D. Maher, B. G. Williams, M. C. Raviglione, C. Dye, *Arch. Intern. Med.* **2003**, *163*, 1009.
[2] S. Nwaka, A. Hudson, *Nat. Rev. Drug Discovery* **2006**, *5*, 941.
[3] T. L. Blundell, H. Jhoti, C. Abell, *Nat. Rev. Drug Discovery* **2002**, *1*, 45.
[4] C. W. Murray, D. C. Rees, *Nat. Chem.* **2009**, *1*, 187.
[5] P. J. Hajduk, J. Greer, *Nat. Rev. Drug Discovery* **2007**, *6*, 211.
[6] H. D. H. Showalter, W. A. Denny, *Tuberculosis* **2008**, *88*, S3.
[7] L. Williams, R. Zheng, J. S. Blanchard, F. M. Raushel, *Biochemistry* **2003**, *42*, 5108.
[8] R. Zheng, J. S. Blanchard, *Biochemistry* **2001**, *40*, 12904.
[9] V. K. Sambandamurthy, X. Wang, B. Chen, R. G. Russell, S. Derrick, F. M. Collins, S. L. Morris, W. R. Jacobs, *Nat. Med.* **2002**, *8*, 1171.
[10] A. Ciulli, D. E. Scott, M. Ando, F. Reyes, S. A. Saldanha, K. L. Tuck, D. Y. Chirgadze, T. L. Blundell, C. Abell, *ChemBioChem* **2008**, *9*, 2606.
[11] K. L. Tuck, S. A. Saldanha, L. M. Birch, A. G. Smith, C. Abell, *Org. Biomol. Chem.* **2006**, *4*, 3598.
[12] S. Velaparthi, M. Brunsteiner, R. Uddin, B. Wan, S. G. Franzblau, P. A. Petukhov, *J. Med. Chem.* **2008**, *51*, 1999.
[13] E. L. White, K. Southworth, L. Ross, S. Cooley, R. B. Gill, M. I. Sosa, A. Manouvakhova, L. Rasmussen, C. Goulding, D. Eisenberg, T. M. Fletcher, *J. Biomol. Screening* **2007**, *12*, 100.
[14] A. Ciulli, C. Abell, *Curr. Opin. Biotechnol.* **2007**, *18*, 489.
[15] G. Jones, P. Willett, R. C. Glen, *J. Mol. Biol.* **1995**, *245*, 43.
[16] C. Dalvit, G. Fogliatto, A. Stewart, M. Veronesi, B. Stockman, *J. Biomol. NMR* **2001**, *21*, 349.
[17] A. L. Hopkins, C. R. Groom, A. Alex, *Drug Discovery Today* **2004**, *9*, 430.
[18] M. Lo, A. Aulabaugh, G. Jin, R. Cowling, J. Bard, M. Malamas, G. Ellestad, *Anal. Biochem.* **2004**, *332*, 153.
[19] H. Jhoti, A. Cleasby, M. Verdonk, G. Williams, *Curr. Opin. Chem. Biol.* **2007**, *11*, 485.
[20] S. Chung, J. B. Parker, M. Bianchet, L. M. Amzel, J. T. Stivers, *Nat. Chem. Biol.* **2009**, *5*, 407.
[21] W. L. Delano, The PyMOL Molecular Graphics System, v.0.99, DeLano Scientific, San Carlos, **2002**.

